Jpn. J. Appl. Phys. Vol. 41 (2002) pp. L 351–L 354
Part 2, No. 3B, 15 March 2002

The Spatial Extension of the Field Scattered by Silver Nanoparticles Excited near Resonance as Observed by Apertureless Near-Field Optical Microscopy

Gregory A. WURTZ, Nada M. DIMITRIJEVIC* and Gary P. WIEDERRECHT†
Chemistry Division, Argonne National Laboratory, Argonne, IL 60439, U.S.A.

(Received November 5, 2001; accepted for publication January 30, 2002)

We report an investigation of the field scattered by isolated silver nanoparticles on a glass substrate observed by apertureless near-field optical microscopy with an illumination wavelength of 404 nm. We observe an unexpected spatial extension of the scattered field. The near-field contrast (both distribution and intensity) is shown to be strongly sensitive to polarization of the incident light. A large ($\times 10$) field enhancement observed in transverse magnetic (TM) polarization is interpreted to be the result of the contribution of the particle plasmon resonance to the diffracted field. The results are further discussed in terms of the particle shape and the experimental configuration used. [DOI: 10.1143/JJAP.41.L351]

KEYWORDS: nanoparticle, scattering, SNOM, AFM, plasmon, resonance, silver, ATR

Nanometer-sized metallic particles are of interest for various optical based applications, such as surface enhanced Raman spectroscopy,[1] chemical sensors,[2] and photonic structures.[3,4] Their ability to show marked local field enhancement of the incident electromagnetic field due to plasmon excitation, as well as the sensitivity of this behavior to the particle shape and surrounding physicochemical properties, make metal nanoparticles particularly suited for these applications. While most studies are performed using conventional far-field techniques, the fundamental interactions occur in the vicinity of the particles and are therefore governed by the near-field response of the particles. To gain an understanding of these interactions, several groups are using scanning near-field optical microscopy (SNOM).[4,5] This technique has been developed in the past ten years to overcome the spatial resolution limitations of conventional optical microscopes. These microscopes, classified as scanning probe microscopes, have since proven their utility in various nanoscopic applications. Although their first purpose is to characterize electromagnetic fields or modify matter at sub-wavelength dimensions, they also represent a unique way to understand the interactions between objects and fields on the nanometric scale. A knowledge of these interactions is critical for understanding the unique optical phenomena that can occur in more structured nanometric environments, such as the observation of squeezed plasmons in interacting metal nanoparticles.[4,6] In this study we explore the field diffracted by isolated silver (Ag) nanoparticles excited near resonance in total internal reflection using an apertureless SNOM.[7] Unexpectedly, high spatial extension of the field distribution is observed in both transverse electric (TE) and transverse magnetic (TM) polarizations. Furthermore, we show that the SNOM contrast in TM polarization is significantly affected by multiple scattering between the probe and the field diffracted by the particle.

The sample is obtained by spin coating a colloidal solution of Ag nanoparticles on a borosilicate glass cover slip ($n \sim 1.55$). The spherical colloidal Ag particles are prepared according to ref. 8 using sodium polyphosphate as a stabilizer. The spin-coating process allows us to efficiently isolate particles on the substrate according to their size. Our experiments were performed on particles with diameters ranging from 20 to 50 nm.

The experimental configuration for this study is shown in Fig. 1 and is similar to that described in ref. 9 except for the illumination conditions. For our experiments, the spin-coated sample is coupled to the dove prism ($n \sim 1.53$) using immersion oil ($n \sim 1.52$). The nanoparticles are far-field illuminated by an evanescent wave obtained by a slightly focused 1mW laser diode beam which undergoes total internal reflection at the sample/air interface (incidence angle $\theta_i = 50°$). The excitation wavelength of 404 nm lies in the resonance bandwidth of the colloidal solution. A half-wave plate controls the incident polarization; the polarization ratio was measured to be about 400 : 1 at the prism entrance facet. The 10^{-4} cm^2 illuminated area results in a 10 W/cm^2 power density on the sample surface.

To characterize the distribution of the field diffracted by the particles we used a commercially available silicon tip (NCH-W, Nanosensors). An atomic force feedback loop (Multimode/Nanoscope IIIa controller, Digital Instruments) ensured a constant probe to sample distance regulation in the tapping mode. An optical fiber (0.2 NA, 100 μm core) at an angle of 75° from the probe axis partially collects the field radiated by the probe in the backscattering direction with respect to the incident wave vector (see Fig. 1). The output of the fiber reaches a photomultiplier tube (Hamamatsu H5773-01) via an interference filter centered at 400 nm and is lock-in demodulated to provide the SNOM signal. The results presented in this paper were obtained with a probe vibration amplitude of 75 nm and lock-in detection at the probe vibration frequency of $\sim$300 kHz. We note here that a complete characterization of the field diffracted by the particles would imply the necessity for further analysis of the radiation pattern of the probe.[10]

Figure 2(a) represents the atomic force microscopy (AFM) image of two isolated Ag particles. Figures 2(b) and 2(c) present the near-field contrast associated with these particles in TE and TM polarizations, respectively. For the sake of clarity in the SNOM images and unless otherwise stated, 15×15 μm scans are presented throughout the paper and the data are also shown in their 3D representation when relevant. The size of the Ag particles (27 and 40 nm) has been determined precisely from 0.5×0.5 μm^2 AFM images.

*Present address: Chemical Technology Division, Argonne National Laboratory, Argonne, IL 60439, U.S.A.
†E-mail address: wiederrecht@anl.gov

The field distribution around the particles illuminated in TE polarization (Fig. 2(b)) represents the mesoscopic scattering of these particles as predicted theoretically.[5,11] In particular it shows the specific 'V'shape in the forward scattering direction (to the left) as well as fringes developing on both sides of the particles (indicated by arrows in Fig. 2(b)) that result from the interference between the field scattered by the particles and the incident wave.[12] When the sample is illuminated in TM polarization, the SNOM image reveals a more spatially extended distribution of the field (Fig. 2(c)). This contrast shows an additional pattern to that of Fig. 2(b), with the initial field interfering with a second scattering pattern that extends as long tails in the backscattering direction (to the right). The remarkable difference between TM and TE illumination in the field's spatial distribution, a difference not predicted theoretically, is rooted in the fact that the simulations do not take into consideration the presence of the probe, and thus neglect its contribution to the resulting SNOM contrast. The deviation of the contrast in TM polarization (Fig. 2(c)) from the calculated ones results from multiple scattering occurring between the probe and the particles.[13] The enhanced sensitivity of the probe to fields vibrating along the probe axis[14,15] (the 'lightning rod effect') supports this observation as these tails almost completely disappear in TE polarization, as shown in Figs. 2(b) and 2(b′).

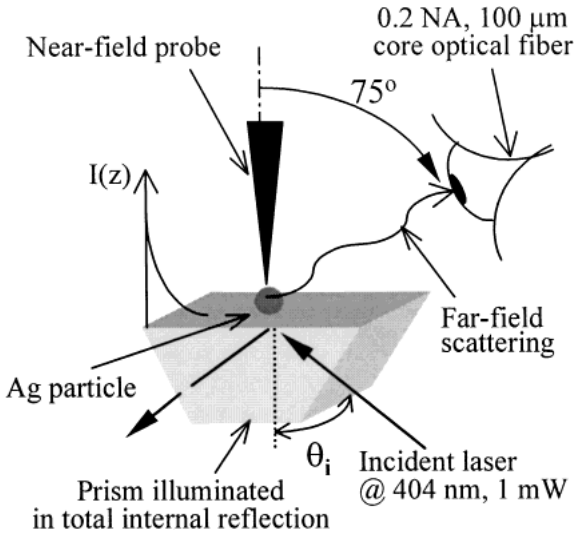

Fig. 1. Schematic of the experimental setup.

In addition to the differences in the spatial distribution of the field revealed in Figs. 2(b) and 2(c), the intensity of the field diffracted by the particles for each incident polarization is significantly different. In TE polarization, the scattered field intensity shows only a slight contrast to the background intensity, whereas a large enhancement ($\sim \times 10$) is observed in the near-field map disturbance produced by the particles in TM

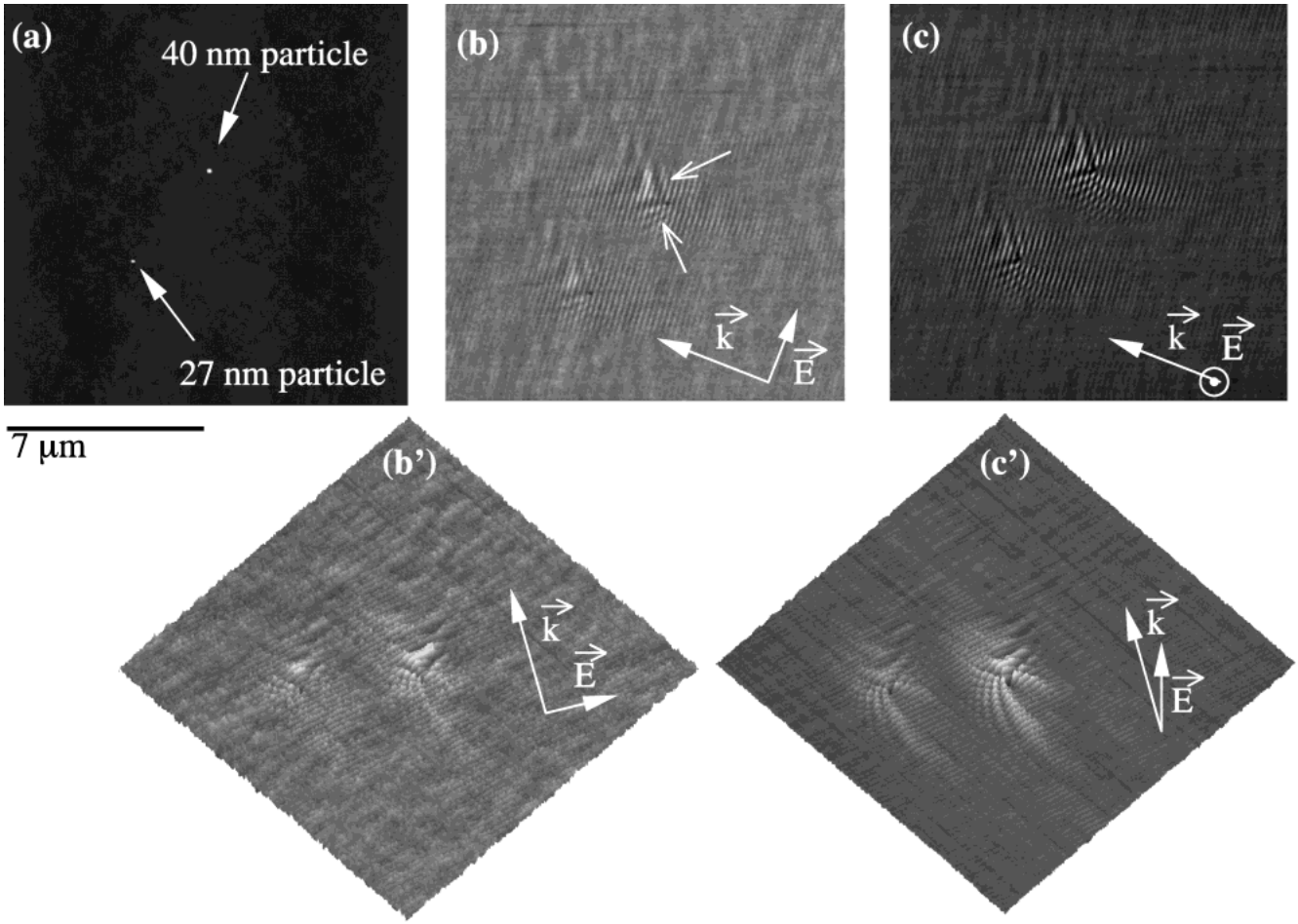

Fig. 2. Isolated Ag nanoparticles illuminated in total internal reflection at $\lambda = 404$ nm on a glass substrate. (a) AFM image of 27- and 40-nm diameter particles. (b) Corresponding SNOM contrast in TE polarization and (c) TM polarization. The scan size of the images is 15 μm. (b′) and (c′) are the 3D representation of (b) and (c), respectively. Arrows in 2(b) highlight the presence of the interference fringes between the particle's scattered field and the incident wave.

polarization. In order to gain more insight into the enhancement mechanism, we studied the field diffracted by comparably sized gold (Au) particles for which the solution plasmon absorption is centered at 530 nm. Figures 3(a) and 3(b) present the AFM and the SNOM images for a 35-nm-diameter Au particle, respectively. A scan size of 6 microns was set for these images. It is evident that the intensity enhancement and the extended spatial distribution of the field, observed for Ag nanoparticles in TM polarization, are not present for Au.

These complementary experiments show that only the Ag particles are resonantly excited, and that the resonance condition has a strong impact on both the intensity and spatial distribution of the SNOM signal. The difference can be seen in Figs. 2(c) and 3(b), where the lightning-rod effect and the large local field around the resonant Ag particle lead to multiple scattering between the Ag particle and the probe. Since the Au nanoparticles are not excited near their plasmon resonance, no significant multiple scattering between the Au particle and the probe is observed. In fact, the near-field contrast from the Au particles in TM polarization (Fig. 3(b)) is comparable in distribution to the contrast obtained for Ag in TE polarization (Fig. 2(b)). This is due to the fact that, in both experiments, only one of the scattering elements (particle or probe) presents an enhanced field. For Fig. 2(b), the probe enhancement is absent due to TE polarization and for Fig. 3(b), the particle field enhancement is absent for Au. Thus, an enhanced field must be present around both the probe and the particle in order to observe the multiple scattering present in Fig. 2(c), a condition only satisfied for TM polarization with resonant Ag particles.

Interestingly, it is also notable that although the far-field illumination polarization in Fig. 3(b) matches the geometrical field enhancement condition at the probe extremity, the optical contrast reflects the scattering diagram of the particle rather than the scattering diagram of the probe.[16] Otherwise, the scattering diagram of the probe as imaged by the particle would be inverted in Fig. 3(b) with respect to the principal scattering direction. However, the probe sensitivity increases for TM-polarized fields like the one diffracted by the Au particle under these illumination conditions. The near-field contrast would in this case reflect the TM component of the field diffracted by the particle, as observed in Fig. 3(b).

Since small metallic particles are expected to exhibit a highly confined enhanced field when excited upon resonance,[4,11,17,18] the marked spatial extension of the field illustrated in the SNOM images is of interest. Although our measurements reveal a large enhancement due to the particle resonant excitation (Fig. 2(c)), the expected spatial confinement has not been observed. To clarify our results, we emphasize two effects that may explain this behavior:

i. Both enhancement and spatial confinement are closely related: the field enhancement increases significantly as the particle symmetry decreases.[18] Going from spherical to square to triangular shape, the geometrical singularities of nonspherical particles contribute to the strong spatial confinement of the field as observed in refs. 4,11,17,18. In our case, the spherical particles studied do not present any electric singularity that could lead to such a confinement. Our measurements would thus be less sensitive to the field diffracted by the extreme part of the tip, and the scattering of a larger part of the tip body would contribute to the contrast in the images presented here. However, it must be noted that these results do not contradict the subwavelength characterization of the field depicted in Figs. 2(b), 2(c) and 3(b).

ii. The experimental configuration used in this study (see Fig. 1) restricts our analysis to the field diffracted by the probe within a given solid angle defined by the collection fiber. Although we have observed that the near-field contrast is strongly sensitive to the angle formed by the probe axis and the collection fiber axis, no spatial confinement has been observed. This sensitivity is illustrated in Fig. 4, by the AFM (Fig. 4(a)) as well as the typical SNOM contrast (Fig. 4(b)) obtained for a far-field detection performed at a grazing angle (fiber axis at 90° from the near-field probe axis in Fig. 1). The contrast is related to the imaging of a 44-nm-diameter Ag particle illuminated in TM polarization. Figure 4(b) represents a complementary component of the field distribution shown by Fig. 2(c) and is believed to describe the propagating component of the scattering diagram of the probe illuminated by the Ag particle excited resonantly.[16] Although further experiments are needed to better clarify this spatially extended contrast, it is clear from Fig. 4(b) that the resonance excitation of the silver nanoparticle produces a markedly enhanced field. A similar experiment conducted by Hamann *et al.* on gold particles[19] showed a high spatial confinement of the field in the particle vicinity, by investigating a complementary solid angle not yet accessible in our configuration.

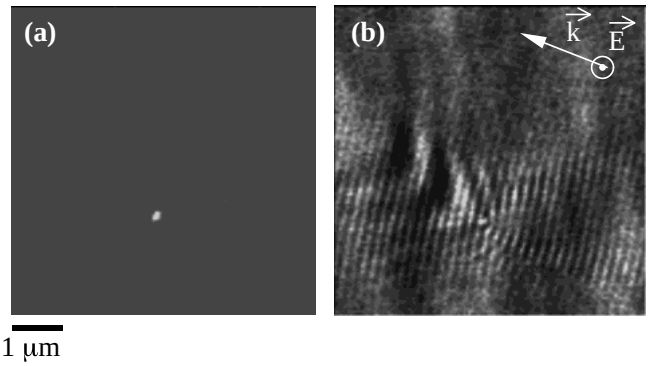

Fig. 3. Isolated Au nanoparticle illuminated in total internal reflection at $\lambda = 404$ nm on a glass substrate. (a) AFM image of a 35 nm diameter particle. (b) Corresponding SNOM contrast in TM polarization. The scan size in the images is 6 μm.

In summary, we studied the near-field distribution of the field scattered by isolated Ag nanoparticles using apertureless SNOM. The response of the Ag particles shows a large enhancement in TM polarization, signifying the importance of the particle's plasmon resonance to both distribution and intensity of the scattered field imaged under these excitation conditions. The spatial distribution of the scattered field has been shown to extend well beyond the topographical limits of the particles. Both the particle shape and experimental considerations have been discussed in order to explain this behavior.

This work was supported by the US Department of Energy, Office of Basic Energy Sciences, Division of Chemical Sciences under contract number W-31-109-ENG-38. We gratefully acknowledge useful discussions with George Crabtree, David Gosztola, Marion Thurnauer, Alexander

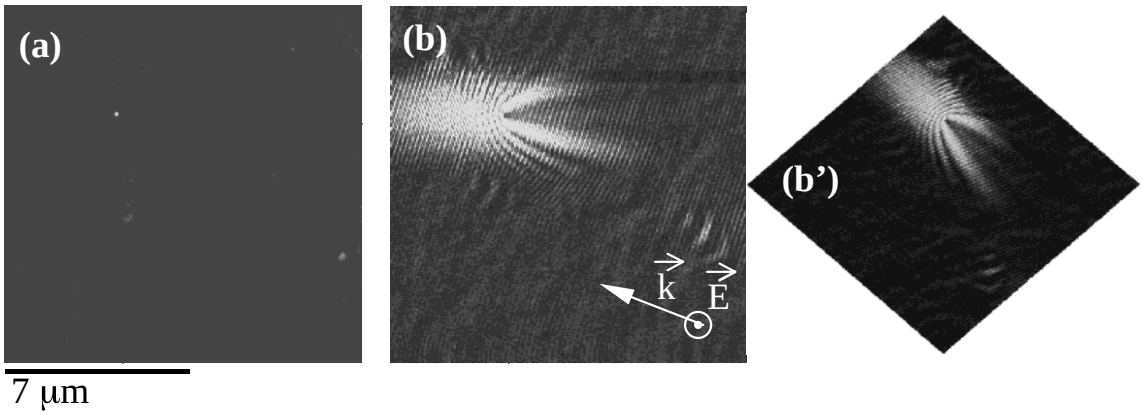

Fig. 4. Isolated Ag nanoparticle illuminated in total internal reflection at $\lambda = 404$ nm on a glass substrate. (a) AFM image of a 44-nm-diameter particle. (b) Corresponding SNOM contrast in TM polarization. (b′) is a 3D representation of (b). The far-field detection fiber collects the field scattered by the tip at a grazing angle. The scan size of the images is 15 μm.

Trifunac, and Ulrich Welp. This work also benefited from the University of Chicago-Argonne National Laboratory Consortium for Nanoscience Research.

1) M. Moskovits: Rev. Mod. Phys. **57** (1985) 783.
2) R. Elghanian, J. J. Storhoff, R. C. Mucic, R. L. Letsinger and C. A. Mirkin: Science **277** (1997) 1078.
3) M. Quinten, A. Leitner, J. R. Krenn and F. R. Aussenegg: Opt. Lett. **23** (1998) 1331.
4) J. R. Krenn, A. Dereux, J. C. Weeber, E. Bourillot, Y. Lacroute, J. P. Goudonnet, G. Schider, W. Gotschy, A. Leitner, F. R. Aussenegg and C. Girard: Phys. Rev. Lett. **82** (1999) 2590.
5) L. Salomon, C. Charbonnier, F. de Fornel, P. M. Adam, P. Guérin and F. Carcenac: Phys. Rev. B **62** (2000) 17072.
6) M. L. Brongersma, J. W. Hartman and H. A. Atwater: Phys. Rev. B **62** (2000) R16356.
7) M. A. Paesler and P. J. Moyer: *Near-Field Optics* (John Wiley, New York, 1996).
8) V. Vukovic and J. M. Nedeljkovic: Langmuir **9** (1993) 980.
9) B. B. Akhremitchev, S. Pollack and G. C. Walker: Langmuir **17** (2001) 2774.
10) J. N. Walford, J. A. Porto, R. Carminati, J.-J. Greffet, P. M. Adam, S. Hudlet, J.-L. Bijeon, A. Stashkevich and P. Royer: J. Appl. Phys. **89** (2001) 5159.
11) N. Richard: Phys. Rev. E **63** (2001) 26602.
12) The reader can observe the presence of 200 nm spacing fringes in the near-field images. These fringes, oriented perpendicular to the far-field evanescent wave propagation vector, are far-field related and will be discussed elsewhere.
13) P. R. Auvil, J. B. Ketterson, Y. K. Kim and A. Kryukov: Appl. Opt. **37** (1998) 8448.
14) E. J. Sanchez, L. Novotny and X. S. Xie: Phys. Rev. Lett. **82** (1999) 4014.
15) H. Furukawa and S. Kawata: Opt. Commun. **148** (1998) 221.
16) F. H'dhili, R. Bachelot, G. Lerondel, D. Barchiesi and P. Royer: Appl. Phys. Lett. **79** (2001) 4019.
17) J. P. Kottmann, O. J. Martin, D. Smith and S. Schultz: Opt. Exp. **6** (2000) 213.
18) J. P. Kottmann, O. J. F. Martin, D. R. Smith and S. Schultz: Chem. Phys. Lett. **341** (2001) 1.
19) H. F. Hamann, A. Gallagher and D. J. Nesbitt: Appl. Phys. Lett. **73** (1998) 1469.